Three dimensional shear wave scattering MR elastography.

S. Papazoglou[1], S. Hirsch[1], D. Klatt[1], J. Braun[2], and I. Sack[1]
[1]Department of Radiology, Charité University Medicine, Berlin, Berlin, Germany, [2]Institute of Medical Informatics, Charité University Medicine, Berlin, Berlin, Germany

Introduction: Magnetic resonance elastography (MRE) is a non invasive method that combines externally applied vibrations with the motion sensitivity of MRI to measure the shear elasticity soft tissues [1]. In MRE this is traditionally achieved by solving an inverse problem with MRE shear wave images as input data [2]. A complementary approach, which does not require the solution of an inverse problem, is based on an analysis of the distribution of shear wave intensity inside measured MRE wave images. The sensitivity of this intensity speckle analysis with respect to shear wave scattering was previously studied for the case of scalar waves in a two dimensional (2D) scenario of shear horizontal waves [3].

Problem: Shear waves in heterogeneous media are subject to complex scattering and mode conversion. An extension of 2D scatter based MRE to the full 3D vector field is required for estimating the order of scatter effects occurring in biological heterogeneous media. The wave intensity has to be evaluated at a large number of positions in order to allow for statistical effects.

Objective: We present a feasibility study of 3D shear wave scattering MRE on three tissue-mimicking phantoms: i) agar gel as reference phantom (no scattering occurs) ii) agar-starch mixture for inducing shear wave scattering on a microscopic level and iii) agar-starch mixture and small Polyamide (PA) spheres for microscopic and macroscopic scattering. Shear wave scattering is studied in terms of the shear wave intensity distribution.

Theory: In strongly heterogeneous media interference of scattered shear waves leads to pronounced local intensity variations. Shear wave intensity images display fluctuations on scales related to the average distance the shear waves can propagate before being scattered [4]. Since these speckles govern the distribution $P(I)$ of intensity I normalized to its mean value inside the region of interest, they open the perspective to study scattering by MRE. In case of no scattering and an ideal plane wave one will observe a $P(I)$ with only a single peak at unity. In contrast, the more scattering occurs, the broader the distribution $P(I)$ will be, i.e. large deviations from the mean intensity will be more likely to occur.

Methods: Experiments were run on a standard 1.5 T clinical MRI scanner (Sonata, Siemens, Erlangen, Germany). A cradle extended-piston driver was used for f = 100, 125, 150, 175 and 200 Hz harmonic stimulation of the phantom container. A single-shot spin-echo EPI sequence was used for acquiring three orthogonal components of the displacement field in 50 adjacent transversal slices and four time steps over the vibration period. Voxel size was 1.5x1.5x1.5 mm^3 and motion encoding gradients were driven at the external vibration frequency. Three different gel phantoms were fabricated. One phantom was composed solely of Agar-based gel. In two more two phantoms 7.7g cornstarch (per 100 ml water) was added in order to obtain a viscous consistency at high temperature. Approximately 6000 PA beads (nylon, 1.5 mm radius) were added to one of the phantoms as macroscopic scatterers, corresponding to approximately 7% of the total volume. After mixing the beads maintained their positions during solidification of the agar. For data analysis an individual planar region of interest (ROI) was chosen for every slice, such that artefacts from the boundaries, e.g. due to accumulated water, were suppressed. The absolute squares of the orthogonal displacement components inside the volume delimited by the ROIs were summed yielding the shear intensity. Total number of positions at which intensity was evaluated was on the order of 10^5 in each phantom. The intensity was normalized with respect to its mean value inside this volume. Finally, the intensities were binned to yield $P(I)$.

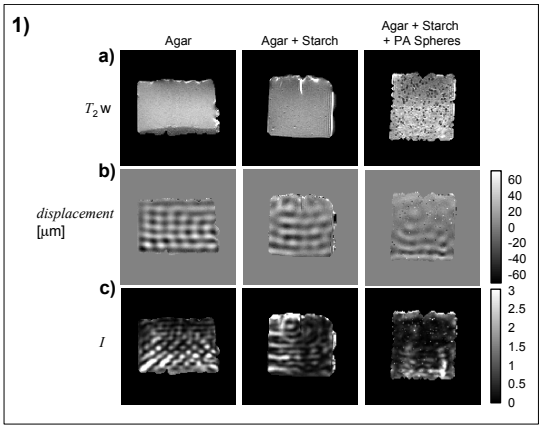

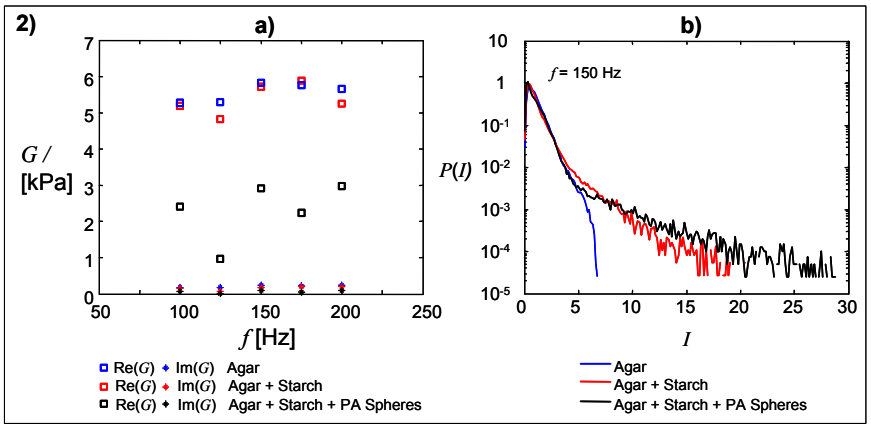

Results: The principal results of this study are presented in figures 1 and 2. Figure **1a)** shows magnitude images of transversal slices through the three investigated phantoms. The PA beads are clearly visible as hypointense spots. The second row **1b)** shows the corresponding displacement fields at 150 Hz excitation frequency (here encoded in the wave component direction through plane). Waves induced from the bottom of the container interfere with waves from the walls. **1c)** displays the corresponding intensity images calculated from all Cartesian wave components. The complex shear modulus determined by a 3D direct inversion algorithm on basis of the Helmholtz equation is shown in figure **2a)**. While scattering from the PA beads leads to a significant reduction of the real part of G, the pure Agar phantom and the Agar+Starch phantom display the same values within accuracy. Figure **2b)** shows $P(I)$ at 150 Hz vibration frequency. As is expected due to the presence of the beads, the broadest distribution is found in the Agar+Starch+PA beads phantom. However, while G suggests similar elastic properties of the Agar and the Agar+Starch phantom, a significant difference is observed in $P(I)$. The Agar+Starch phantom displays much larger intensity fluctuations than the pure Agar phantom suggesting a strong influence due to shear wave scattering from heterogeneities resulting from the additional starch.

Discussion and Conclusion: The feasibility of 3D shear wave scattering MRE was studied in gel phantoms. The results demonstrate that scatttering is clearly visible in the intenstiy distribution. This intensity distribution reveals structural differences even when a wave inversion suggests similar elastic properties. Hence, the variance of normalized intensity fluctuations measured with 3D shear wave scattering MRE provides a useful complementary parameter to standard wave inversions. Further phantom studies and simulations are required to elucidate on the relation between intensity fluctuations and characteristic length scales.

References:

[1] Muthupillai R., Rossman P.J., Lomas D.J., Greenleaf J.F., Riederer S.J., Ehman R.L., *Magn. Reson. Med.*, **36**, 266-274, 1996.
[2] Park E., Maniatty A.M., *Phys. Med. Biol.*, **51**, 3697-3721, 2006.
[3] Papazoglou S., Klatt D., Braun J., Sack I., *Europhys. Lett.*, **91**, 17007p1-p6, 2010.
[4] Van Rossum M.C.W., Nieuwenhuizen Th.M., *Rev. Mod. Phys.*, **71**, 313-371, 1999